Available online at www.sciencedirect.com

SciVerse ScienceDirect

journal homepage: www.elsevier.com/locate/he

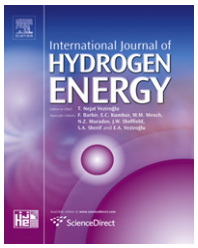

Deposition of Pt nanoparticles on different carbonaceous materials by using different preparation methods for PEMFC electrocatalysts

Natalia Veizaga [a,*], *José Fernandez* [b], *Mariano Bruno* [c], *Osvaldo Scelza* [a], *Sergio de Miguel* [a]

[a] *Instituto de Investigaciones en Catálisis y Petroquímica (INCAPE), Facultad de Ingeniería Química, Universidad Nacional del Litoral, CONICET, Santiago del Estero 2654, 3000 Santa Fe, Argentina*

[b] *PRELINE, Facultad de Ingeniería Química, Universidad Nacional del Litoral, CONICET, Santiago del Estero 2829, 3000 Santa Fe, Argentina*

[c] *Departamento de Física de la Materia Condensada, Centro Atómico Constituyentes, Comisión Nacional de Energía Atómica (CNEA), General Paz 1499, 1650 Buenos Aires, Argentina*

ARTICLE INFO

Article history:
Received 26 June 2012
Received in revised form
28 August 2012
Accepted 29 August 2012
Available online 27 September 2012

Keywords:
Fuel cell
Pt–carbon catalysts
Vulcan carbon
Carbon nanotubes
Mesoporous carbon

ABSTRACT

The objective of this study is to evaluate different methods to obtain Pt (20 wt%)/carbon electrocatalysts, in order to identify the conditions that lead to electrocatalysts with the best electrochemical performance. This paper involves the study of different methods for the deposition and reduction of H_2PtCl_6 on three carbon supports: Vulcan carbon, Multiwall carbon nanotubes and mesoporous carbons. The deposition–reduction methods in liquid phase were carried out with HCOOH or $NaBH_4$ as reducing agents. Besides, the conventional impregnation was carried out by deposition of H_2PtCl_6 on carbon followed by a reduction with H_2 at high temperature. The electrochemical performance of supported Pt catalysts prepared by reduction in liquid phase is strongly dependent on the metallic dispersion, the particle size distribution and the nature of the carbonaceous material used as a support. Results show that the deposition–reduction method using HCOOH 0.3 M at 50–60 °C and a mesoporous carbon leads to the most efficient electrocatalyst.

1. Introduction

Proton exchange membrane fuel cell (PEMFC) is one of the most promising alternative power sources for several applications due to its high energy conversion efficiency and low pollution. Some challenges still exist, for example, performance should be further improved and its cost must be reduced for commercialization. These depend, between other factors, on the increment in the activity of electrocatalysts and Pt utilization [1,2].

Catalysts for PEMFC are basically composed of platinum nanoparticles deposited on a carbon conducting support. The size and distribution of these nanoparticles have an influence on the apparent activity of the electrode for both the hydrogen oxidation (HOR) and the oxygen reduction (ORR) reactions when these catalysts make a membrane electrode assembly (MEA) of PEMFC [3–5].

Different reduction methods of the platinum precursor (usually chloroplatinic acid), which differ in the reduction agent employed, have been described in the literature, including the formic acid [6–8], sodium borohydride [9,10], ethylene glycol–water solution [11], hydrazine [12], formaldehyde [13], the impregnation method followed by reduction with hydrogen at high temperature [14] and the microwave-

* *Corresponding author*. Tel.: +54 (342) 4555279; fax: +54 (342) 4531064.
E-mail address: nveizaga@fiq.unl.edu.ar (N. Veizaga).

0360-3199/$ – see front matter
http://dx.doi.org/10.1016/j.ijhydene.2012.08.144

assisted method in ethylene glycol [8,15]. Nores Pondal [16] indicates that catalysts prepared by reduction with formic acid and ethylene glycol (microwave-assisted) show electrochemical activities very close to those of the commercial catalyst, and are almost insensitive to the Pt dispersion or Pt particle size. Zhang et al. [12] pointed out that the catalytic activity for oxygen reduction increases in the order: Pt(HCOOH) > Pt($NaBH_4$) > Pt(N_2H_4). One problem associated with the reduction in liquid phase is the reducibility degree of the metallic precursor [17]. When the reduction is carried out by using H_2, the reducibility and the dispersion of the metal can be defined by the reduction temperature [14]. Xing [11] presents a sonochemical technique for the treatment of carbon nanotubes that allows deposition of highly dispersed high loading Pt nanoparticles on them. Compared to previous techniques for the treatment of carbon nanotubes, the sonochemical technique is able to functionalize most of the carbon nanotubes by preventing them from forming aggregates during the treatment process.

The electrochemical performance of these carbon-supported electrodes depends in an important degree on the deposition–reduction method and the nature of the support. Not only the metallic dispersion and distribution of metallic sizes could be the fundamental factors that affect the electrochemically active specific surface (EASS) but also the nature of the support.

It is very important to note that there are no systematic and comparative studies of the deposition–reduction methods and the influence of these methods on the physicochemical characteristics of the metallic phase and on the EASS of the whole electrode. It should be noted that, for a particular active material, the EASS area is the key parameter that dominates the apparent electrocatalytic activity of the material for a certain reaction. Hence the aim of this paper is to study the incidence of the different preparation methods and the optimization of the different preparation variables in order to obtain catalysts with a better electrochemical performance. Besides, the use of non-conventional supports like a mesoporous carbon synthesized in CNEA (National Commission of Atomic Energy, Argentina) is very important for this study [18,19]. Hence a systematic study on the method of deposition–reduction of Pt supported on different carbonaceous materials (carbon Vulcan, mesoporous carbon and carbon nanotubes) with different reducing agents in liquid phase was carried out. Moreover the results obtained by this method were compared with those obtained by conventional impregnation with H_2PtCl_6 and further reduction with H_2. The used characterization techniques were TPR, XRD, XPS, TEM, H_2 chemisorption and voltammetric CO stripping.

2. Experimental

2.1. Preparation of the electrocatalysts

The carbonaceous supports used for the catalyst preparation were: (i) carbon Vulcan (VC); (ii) multiwall carbon nanotubes (NT); (iii) mesoporous carbon (MC) (see Table 1). Vulcan carbon XC-72 has a specific surface area (S_{BET}) of 240 $m^2\ g^{-1}$, a pore volume (V_{pore}) of 0.31 $cm^3\ g^{-1}$ and a mean particle size of 40 nm. A commercial multiple wall carbon nanotube (MWCN from Sunnano, purity >90%, diameter: 10–30 nm, length: 1–10 μm) with the following textural properties: S_{BET} = 211 $m^2\ g^{-1}$, V_{pore} = 0.46 $cm^3\ g^{-1}$, was used. The physical properties of the mesoporous carbon, were: S_{BET} = 476 m^2/g, V_{pore} = 0.35 $cm^3\ g^{-1}$. The total pore volume (at p/p^0 = 0.986) is 0.99 $cm^{-3}\ g^{-1}$ and the micropore volume deduced by DR was 0.23 $cm^{-3}\ g^{-1}$. A maximum in the pore size distribution is found at around 9 nm (see Fig. 1). The micro- (<2 nm) and meso-porosity (between 2 and 50 nm) is attributed to the structure of the carbon, which consists of clusters of porous uniform spheres in a fairly regular array. Therefore, the obtained material has a hierarchical pore structure (micro- and meso-porosity) [18,19].

Table 1 – Physical properties and impurities of the supports.

Support	S_{BET} ($m^2\ g^{-1}$)	V_{pore} ($cm^3\ g^{-1}$)[a]	Impurities
Vulcan XC-72	240	0.31	Al, Si, C, Mg, K and Zn, S: negligible
Carbon nanotubes	211	0.46	Fe: 2%; Al: 1.5%; Si, S, Ca: negligible
Mesoporous carbon	476	0.35	Cl: 0.3%; S: negligible

a V_{pore}: total pore volume.

The catalysts were prepared by two methods: (a) deposition–reduction in liquid phase using HCOOH (called RF) (Cicarelli, analytical grade) or $NaBH_4$ (called RB) (Merck, analytical grade) as reducing agent, and (b) conventional impregnation (called CI) in aqueous medium with H_2PtCl_6 (Tetrahedron, A.C.S. Reagent). In all cases the Pt content was 20 wt%.

Pt(20 wt%)/VC catalysts were prepared by using different HCOOH concentrations (0.1 M, 0.2 M, 0.3 M and 0.5 M) with the object to find the optimal concentration of HCOOH that lead to smaller Pt particle sizes. For the preparation of catalysts on the other supports (carbon nanotubes and mesoporous carbon) it was used the optimal concentration of the reductive agent previously determined on Pt/VC catalyst. In the preparation of Pt/VC catalyst by deposition–reduction with formic acid, a suspension of the support and formic acid was prepared (1 g of VC and 50 mL of formic acid of appropriate concentration) by sonication at room temperature for 15 min. The suspension was thermostated under stirring (300 rpm) at 50–60 °C for 30 min. The formic acid reduction consists on the addition of the H_2PtCl_6 solution in three steps under stirring. The contact time for each addition of H_2PtCl_6 was at least 2 h. After 1 h of the first addition of the Pt precursor, 10 mL of formic acid was added in order to assure the total reduction of the metallic compound. After each H_2PtCl_6 addition, a reducibility test was carried out by using KI and starch (indicator) following the technique reported by Nores Pondal [16].

If the liquid sample remains colorless, this means that all Pt is reduced to metallic state. On the contrary, if the solution was not colorless, more HCOOH was added and the reducibility test was carried out again. This procedure was repeated until a colorless liquid was obtained. After addition of the three portions of H_2PtCl_6, the sample was filtered and the solid

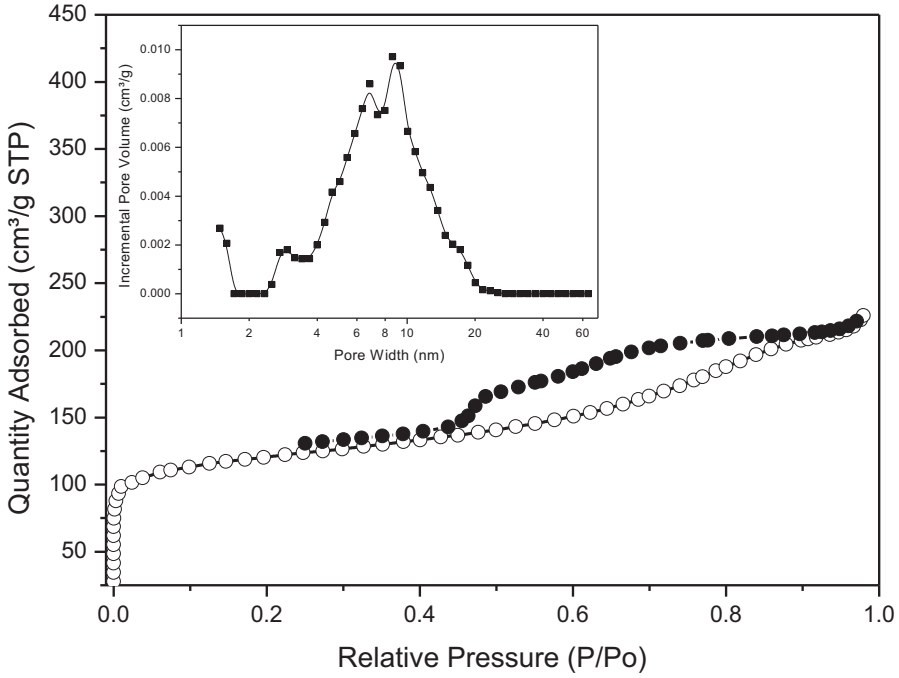

Fig. 1 – Nitrogen adsorption–desorption isotherms and pore size distribution corresponding to the mesoporous carbon.

was washed with distilled water. In the case of catalysts prepared by deposition–reduction in liquid phase (formic acid or sodium borohydride) the reduction occurred preferentially on the surface of the carbon support and, when it was completed, the suspension was cooled down up to room temperature and finally the catalyst was filtered and dried in vacuum at 50 °C for 3 h.

When the reductive sodium borohydride method is applied, solutions of different concentrations of $NaBH_4$ (0.2, 0.4 and 0.6 M) in 1 M NaOH were used. There is a difference in the procedure with respect to that of the formic acid since the addition of H_2PtCl_6 was made in one step, and the reductive agent was added in four portions of the same volume. The portions were added after 30 min one from the other. The reducibility test was carried out before the next $NaBH_4$ addition. The catalyst was finally filtered, washed with distilled water and dried under vacuum at 50 °C for 3 h.

The conventional impregnation (CI) method consists on the impregnation of the support with the metallic precursor (H_2PtCl_6) followed by a reduction step with flowing H_2. The impregnation was carried out under stirring (400 rpm) using an impregnation volume/mass of support ratio of 30 mL g^{-1}. The amount of Pt added to the support was such as to obtain a final Pt loading in the final catalyst of 20 wt%. The impregnation time was 8 h at room temperature. After impregnation the overall sample (solid and the remaining liquid) was dried a 120 °C for 12 h, in order to assure the total deposition of the metallic precursor. After drying, the catalyst precursor was reduced with a H_2 flow (heating rate = 8 °C min^{-1}) at 230 °C for 2 h [14].

2.2. *Characterization of the Pt/C electrocatalysts*

The H_2 chemisorption measurements were made in a volumetric equipment at room temperature. The sample weight used on the experiments was 0.100 g, previously outgassed under vacuum (10^{-4} Torr). The H_2 adsorption isotherms were performed at room temperature between 25 and 100 Torr. The isotherms were linear in the range of used pressures and the H_2 chemisorption capacity was calculated by extrapolation of the isotherms to zero pressure [20]. In the case of catalysts obtained by CI the sample was previously reduced under H_2 flow at 230 °C for 2 h. Then the sample was outgassed under vacuum at the same temperature, finally cooled down to room temperature before the H_2 chemisorption.

The catalysts (previously dried at 120 °C) were also characterized by temperature-programmed reduction (TPR) by using a reductive mixture (10 mL min^{-1}) of H_2 (5% v/v)–N_2 in a flow reactor. The samples were heated at 6 °C min^{-1} from 25 up to 800 °C. The outlet of the reactor was passed through a TCD detector in order to obtain the TPR signal.

XPS determinations were carried out in a Multitechnic Specs photoemission electron spectrometer equipped with an X-ray source Mg/Al and a hemispherical analyzer PHOIBOS 150 in the fixed analyzer transmission (FAT) mode. The spectrometer operates with an energy power of 100 eV and the spectra were obtained with a pass energy of 30 eV and a Mg anode operated at 90 W. The pressure of the analysis chamber was kept a pressure lower than 1.5×10^{-8} Torr. The binding energies (BEs) of the signals were referred to the C1s peak at 284 eV. Peak areas values were estimated by fitting the curves with combination of Lorentzian–Gaussian curves of variable proportion and using the CasaXPS Peak-fit software version 1.

The catalyst samples were also analyzed by X-ray diffraction (XRD) techniques. X-ray diffraction experiments were performed at room temperature in a Shimadzu model XD3A instrument using CuKα radiation (λ = 1.542 Å) generated at 30 kV and current of 40 mA that swept between 20 and 100θ.

Transmission electron microscopy (TEM) measurements were carried out on a JEOL 100CX microscope, operated with an acceleration voltage of 100 kV, and magnification ranges of 80,000× and 100,000×. For each catalyst, a very important number of Pt particles (approximately 200) were observed and the distribution of particle sizes was done on this basis. The mean particle diameter (d) was calculated as: $d = \Sigma(ni \cdot d_i)/\Sigma ni$; ni: number of particles of diameter d_i.

The electrochemical characterization of the catalysts was performed by cyclic voltammetry in a conventional three-electrode cell, using a potentiostat/galvanostat (TEQ-02, Argentina). The working electrode consisted of an active layer made with a suspension blended from 10 mg of Pt/C, 40 μL of Nafion solution (5 wt%, Aldrich) and 80 μL of iso-propyl alcohol. After homogenization in an ultrasonic bath (30 min), 10 μL of this suspension was deposited on a glassy carbon electrode (area 0.2 cm^2) previously polished with alumina paste (Micropolish) up to 1 μm, and washed with ethanol–water solution. The resulting layer was dried in an oven at 60 °C for 30 min to ensure its binding to the glassy carbon rod. All experiments were carried out at 30 °C. The counter-electrode was a Pt foil and an Ag/AgCl (in 3 M NaCl) electrode was employed as a reference. In order to decrease contamination with chloride and silver due to possible leakage of the reference electrode, this electrode was placed inside a separate compartment that was connected to the cell through a Luggin-Haber capillary. In addition, the capillary end was positioned in close proximity to the working electrode to avoid ohmic drops during measurements. The electrochemical area was quantified by measuring the charge for the electro-oxidation of adsorbed CO (or CO stripping) [21]. Before this experiment, the working electrode was repeatedly scanned between −200 and 1200 mV vs. Ag/AgCl at a sweep rate of 100 mV/s in a 0.5 M H_2SO_4 solution, to assure the stabilization of the catalyst layer response. The adsorption of a CO monolayer on the electrode catalyst was carried out by bubbling carbon monoxide (10% v/v CO in N_2) through the electrolyte (H_2SO_4 0.5 M) for 2 h, while the electrode potential was kept at a constant value of 200 mV vs. Ag/AgCl. Then the solution was purged with N_2 for 20 min to remove the residual CO from the solution. In order to observe the actual process of liberation of the Pt active sites, the potential was scanned from 200 mV to 1200 mV vs. Ag/AgCl in N_2, and then cycled in the range −200 mV $\leq E$ (vs. Ag/AgCl) $\leq$1200 mV. The electrochemically active area of Pt was estimated by calculation of the charge for CO oxidation by integrating the peak of the first sweep, as will be detailed later.

3. Results and discussion

3.1. Catalyst characterization

Temperature-programmed desorption experiments were used to characterize the surface oxygen groups (carboxylic, anhydride, lactone, phenol, carbonyl groups, etc.) [22] of different carbons. Carboxylic and anhydride groups are considered as strong acid ones, while lactone, phenol and carbonyl groups display weaker acid properties. It has been reported [23,24] that the stronger acid groups lead to a CO_2-desorption at low temperatures during TPD experiments, in contrast with the weaker acid sites which lead to a CO-desorption at higher temperatures. From TPD results (Fig. 2), the VC does not practically show the presence of functional groups on its surface, while the carbon nanotubes display the desorption of very low amounts of weak acid functional groups at high temperatures. Finally the mesoporous carbon is the support with the highest amounts of functional groups, both at T <500 °C (strong acid sites) and at T >500 °C (weak acid groups). It must be noted that the surface oxygen groups could act as anchorage sites of the metallic precursor [25,26].

In order to study in a systematic way the deposition–reduction method in liquid phase different aspects such as the deposition capacity of the metallic phase on the carbonaceous materials, the reducibility degrees of the active phase and the structure of metallic particles, were investigated.

To study the influence of the formic acid concentration on the characteristics of the deposited Pt nanoparticles, four different concentrations of formic acid (0.1, 0.2, 0.3 and 0.5 M) were studied. It must be noted that the time necessary to reduce the metal during each addition step of the Pt precursor was increasing as the formic acid concentration decreased. In all deposition–reduction (formic acid and sodium borohydride) experiments, before adding the support, the very concentrated chloroplatinic acid solution (necessary to deposit 20 wt% on the support) displayed a dark orange color, whereas after filtering the final suspension, the solution becomes completely transparent. This result would indicate the absence of Pt precursor in the solution. In fact, chemical

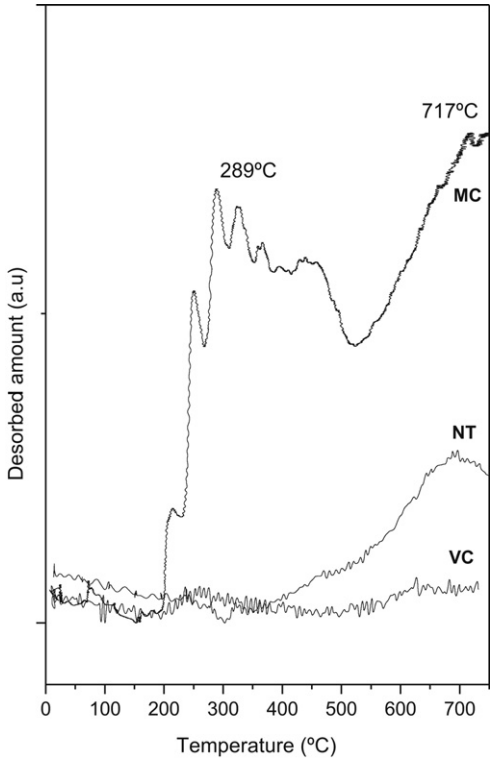

Fig. 2 – TPD profiles for Vulcan carbon (VC), carbon nanotubes (NT) and Mesoporous carbon (MC).

analysis of these solutions after the reductive treatment by the formic acid method showed negligible quantities of Pt, such as Table 2 shows. Hence, the reduction in liquid phase with formic acid for preparing a Pt/VC catalyst guarantees a complete deposition of the metallic precursor on the carbonaceous support. Similar results were found when the concentration of sodium borohydride (reducing agent) was modified between 0.2 and 0.6 M, such as shown in Table 2.

To analyze the reducibility degree of the deposited Pt, TPR experiments were carried out on the catalysts prepared by deposition–reduction in liquid phase with formic acid or sodium borohydride. Fig. 3 shows a comparison of the profiles obtained for the samples prepared by the formic acid method (RF) and one prepared by reduction with $NaBH_4$ (RB), with that obtained by a conventional impregnation technique (CI). This last catalyst prepared by impregnation and further drying had oxidized Pt species. It can be observed (for the Pt/VC. CI sample) a reduction peak at approximately 230 °C corresponding to the reduction of the deposited metal complex, in agreement with previous works dealing with Pt catalysts supported on carbons [27]. The different catalysts prepared by reduction in liquid phase with HCOOH or $NaBH_4$ show a very slight reduction zone at this temperature. Hence these results clearly show that the use of reduction in liquid phase with formic acid or sodium borohydride leads to an almost complete reduction of Pt on the carbon.

XPS results of Pt4f level obtained in catalysts prepared by the reduction with formic acid 0.3 M and sodium borohydride 0.4 M are shown in Fig. 4(a) and (b), respectively, and in Table 3. From the deconvolution of the spectra of the different samples supported on NT and MC, it was obtained one peak at (71.2–71.6) eV for Pt $4f_{7/2}$ and other peak at (74.6–75.0) eV for Pt $4f_{5/2}$. These peaks are assigned to zerovalent Pt [28]. However, other small doublets at (73.7–73.9) eV and (76.3–77.4) eV corresponding to Pt oxides or oxychlorides are also present [28]. It must be noted that for both catalysts supported on VC, the signals corresponding to metallic Pt are shifted toward lower binding energies and they appeared at (70.3–70.6 eV), probably due to a support effect. The shift observed in XPS spectra can be attributed to that the metal–support interaction could modify in different extension (according to the carbonaceous material used) the electronic characteristics of the Pt species [29]. The concentrations of oxidized surface Pt species are lower than 35%, which means that an important amount of Pt surface is in the zerovalent state. It must be noted that the highest concentration of Pt^0 species (78–79%) is present in catalysts supported on carbon Vulcan (see Table 3). Prabhuram et al. [30] showed similar results for Pt/C catalysts prepared by reduction method in liquid phase, since they found by XPS that 60% of Pt is present in metallic state. It must be indicated that TPR profiles display a very small reduction signal, which is indicative of negligible bulk Pt oxide reduction. However, XPS results show a certain fraction of Pt oxide. These facts can be attributed to a surface oxidation of Pt during the storage of the samples. Since XPS analyzes the first outer layer of the deposited metal, the above-mentioned results would be indicative of the presence of surface Pt oxide together with a major fraction of zerovalent Pt. The O/C XPS ratios were reported in Table 3 and it can be observed that O/C ratios are practically unmodified.

Figs. 5 and 6 show the X-ray diffraction patterns for the different catalysts. In all cases, the observed peaks indicate the presence of the face-centered cubic structure (fcc), typical of platinum metal, represented by the (111), (200), (220), and (311) planes, which appear at 2θ of 39.8, 46.3, 67.5 and 81.6°, respectively [31]. The broadening of the diffraction peaks for Pt/VC. RF 0.3 M is indicative of small average crystallite size, as expected from Scherrer equation, and it is also an evidence of lower degree of crystallinity, typical of small metallic particles having high lattice strain. From the line broadening of (111) peak at 2θ of 39.8° by using Scherrer equation after background subtraction, the calculated average size of Pt particles follows the sequence: Pt/VC. RF 0.1 M ≅ Pt/VC. RF 0.2 M ≅ Pt/VC. RF 0.5 M > Pt/VC. RF 0.3 M, as can be seen in Table 4. The tendency observed for catalysts prepared by using sodium borohydride as reducing agent with respect to the Pt average size was: Pt/VC. RB 0.2 M ≅ Pt/VC. RB 0.4 M < Pt/VC. RB 0.6 M (Fig. 6 and Table 4).

The sequence of crystallite sizes obtained by XRD is concordant with the sequence of values of the dispersion (calculated from hydrogen chemisorptions) for the four catalysts supported on VC and prepared by reduction in liquid phase with different formic acid concentrations. In fact, the Pt/VC catalyst prepared with formic acid 0.3 M, which displayed the lowest particle diameter by XRD, has the highest Pt dispersion (39%), such as it is observed in Table 4, whereas the other catalysts supported on VC show lower dispersions and consequently higher crystallite sizes, in agreement with XRD results. It was found that these catalysts prepared by the technique of deposition–reduction with formic acid are very sensitive to an additional thermal treatment with hydrogen,

Table 2 – Pt amounts in the initial solution, final solution and Pt concentrations in the carbon Vulcan for reductions with formic acid and sodium borohydride.

Concentration of reducing agent used in the preparation	Initial Pt amount in the solution (mmol)	Final Pt amount in the solution (mmol)	wt% Pt on VC
0.1 M formic acid	1.03	0.01	19.76
0.2 M formic acid	1.03	Undetectable	19.90
0.3 M formic acid	1.03	Undetectable	19.99
0.5 M formic acid	1.03	Undetectable	20
0.2 M sodium borohydride	1.03	Undetectable	20
0.4 M sodium borohydride	1.03	Undetectable	20
0.6 M sodium borohydride	1.03	Undetectable	20

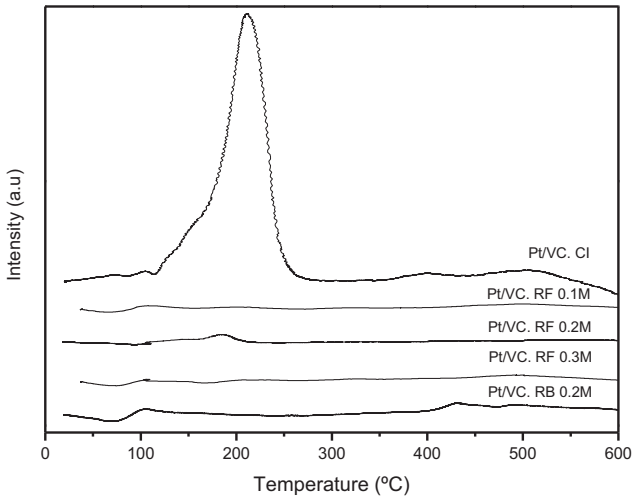

Fig. 3 – TPR profiles of catalysts supported on VC prepared by reduction with formic acid (RF), sodium borohydride (RB) and by conventional impregnation (CI).

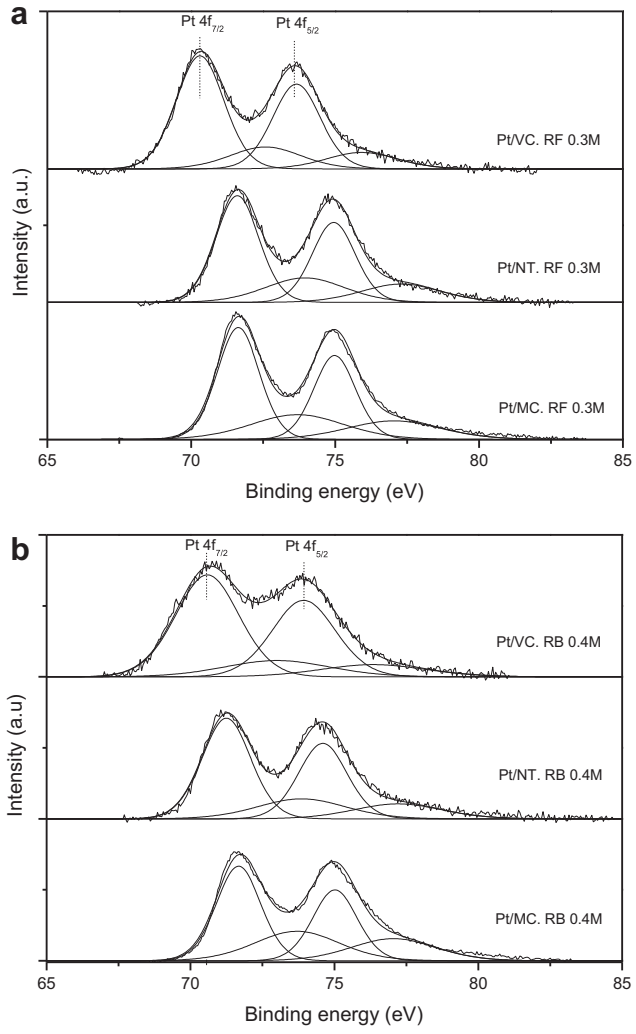

Fig. 4 – XPS results of catalysts prepared by reduction with (a) formic acid 0.3 M and (b) sodium borohydride 0.4 M.

even at relatively low temperatures (100 °C). In fact, all catalysts submitted to a thermal treatment with H_2 at 100 °C displayed an important fall in the metallic dispersion, probably due to a sinterization process that can produce an agglomeration of the metallic particles, favored by the high metallic charges of these catalysts (20 wt%).

From the above-mentioned results it can be concluded that the preparation of Pt/VC samples using a concentration of formic acid equal to 0.3 M leads to catalysts with the highest dispersion which means the smallest crystallite size.

A similar comparative analysis was carried out to select the more appropriate concentration of the other reducing compound ($NaBH_4$) used for the preparation of Pt/VC catalysts. In this sense Table 4 and Fig. 6 show that the use of low concentrations the reducing agent (like 0.2 or 0.4 M) leads to a catalyst with low crystallite sizes and similar dispersion values.

In order to compare the effect of the support (VC, NT and MC) on the Pt crystallite size, the metallic dispersion and the electrochemically active surface area, it was selected a concentration of 0.3 M and 0.4 M for the preparation of Pt catalysts with formic acid and sodium borohydride reductions, respectively (see Figs. 5 and 6 and Table 5). In general, there is a certain relationship between the crystallite size determined by XRD and the metallic dispersion determined by H_2 chemisorption.

The cyclic voltammograms (CVs) corresponding to Pt catalysts prepared by formic acid and sodium borohydride reduction in liquid phase and supported on the three carbonaceous materials are shown in Figs. 7 and 8, respectively. When the Pt surface is blocked by a CO monolayer, the electroadsorption of atomic hydrogen from protons is inhibited. Then, the characteristic peaks of hydrogen adsorption/desorption are not detected in the first scan, but only a sharp peak for oxidation of CO to CO_2 between 600 and 700 mV vs. Ag/AgCl. Once the CO layer is removed by oxidation at high potentials, the adsorption/desorption of hydrogen takes place on the surface of the Pt catalyst and the corresponding peaks appear in the CVs between −200 mV and 200 mV vs. Ag/AgCl. Thus, in the following cycles (between −200 and 1200 mV vs. Ag/AgCl) the classical voltammetric peaks of H adsorption/desorption are observed, which are typical of clean Pt electrodes in N_2-saturated acid solutions.

The electrochemically active specific surface area (EASS) is an important parameter used to compare the electrochemical performance of an electroactive material (in this case Pt) dispersed over a porous non-active support (in this case carbon). Probably the most efficient method for calculation of the electroactive area of a noble metal is the CO stripping by cyclic voltammetry. In this method, the EASS is calculated from the charge for oxidation of a full monolayer of CO adsorbed on the active sites (Q_{CO}) using Eq. (1). The value of Q_{CO} can be obtained from integration of the CO-oxidation peak in the background-subtracted current (i) vs. potential (E) curve, according to Eq. (2), where υ is the scan rate, E_1 and E_2 are the potential limits for integration of the CO-oxidation peak.

$$\mathrm{EASS} = \frac{(Q_{CO}/q^{s}_{CO})}{m_{Pt}} \quad (1)$$

Table 3 – The O/C atomic ratio determined by XPS and the binding energies of the Pt 4f levels for the different catalysts.

Catalyst and preparative methods	Atomic ratio O/C	Species	Binding energy of Pt $4f_{7/2}$ (eV)	Relative population of the species, %
Pt/VC. RF 0.3 M	12.5	Pt^0	70.3	77.6
		Pt^{+2}; Pt^{+4}	72.6	22.4
Pt/NT. RF 0.3 M	11.7	Pt^0	71.6	70.3
		Pt^{+2}; Pt^{+4}	73.9	29.7
Pt/MC. RF 0.3 M	10.2	Pt^0	71.6	67.2
		Pt^{+2}; Pt^{+4}	73.7	32.8
Pt/VC. RB 0.4 M	11.7	Pt^0	70.6	79.1
		Pt^{+2}; Pt^{+4}	73	20.9
Pt/NT. RB 0.4 M	12.6	Pt^0	71.2	73.6
		Pt^{+2}; Pt^{+4}	73.9	26.4
Pt/MC. RB 0.4 M	10.4	Pt^0	71.6	64.8
		Pt^{+2}; Pt^{+4}	73.7	35.2

$$Q_{CO} = \frac{\int_{E_1}^{E_2} i(E)dE}{\upsilon} \quad (2)$$

The parameter q^s_{CO} is the specific charge for the oxidation of CO per platinum area, which is equal to 0.42 mC cm^{-2} (assuming that the surface density of polycrystalline Pt is $1.3 \cdot 10^{15}$ atoms cm^{-2}, that each CO molecule is adsorbed on a single Pt atom, and that two electrons are involved in the oxidation of CO to CO_2). The stripping of CO is a more feasible method than the voltammetric measurements of the hydrogen adsorption charge to determine the EASS areas of Pt nanoparticles when the Pt loading is low. As the CO-stripping peak is sharpener than the peaks for the 1-e^- electrodesorption of adsorbed hydrogen atoms, the subtraction of the capacitive current (proportional to the carbon and platinum area) is much more accurate [32]. The EASS is a magnitude that is referred to the total Pt mass, so the Pt electrochemical area is divided by the weight of Pt (m_{Pt}).

Table 5 shows the values of metallic dispersion, particle diameter calculated from XRD measurements and EASS areas obtained by CO-stripping voltammetry.

Results from Table 5 indicate that the three carbonaceous materials have a different behavior as supports of electrocatalysts. In order to get a better understanding of the results, Fig. 9 correlates the electrochemical area as a function of the metallic dispersion. In this sense, both Pt catalysts supported on carbon nanotubes (which display low dispersion and intermediate EASS values) and those supported on mesoporous carbons (which show both high dispersion and EASS values) follow a certain correlation, while catalysts supported on VC do not follow this behavior, thus displaying good dispersions but low EASS values (see Fig. 9).

With respect to the effect of formic acid or sodium borohydride as reducing agents during the Pt deposition, both of them lead to similar metallic dispersion values and electrochemical areas for each support. However for nanotubes and mesoporous carbons there is a slight increase in the EASS for catalysts prepared by reduction with sodium borohydride.

A similar behavior to that observed in Fig. 9 was found when we tried to correlate the electrochemical area as a function of the particle diameter determined by XRD, such as it is shown in Fig. 10.

Besides, Table 5 also shows the results of metallic dispersions, particle diameters (obtained from XRD) and electrochemical areas (CO-stripping voltammetry) for the catalysts prepared by conventional impregnation (CI). It is observed

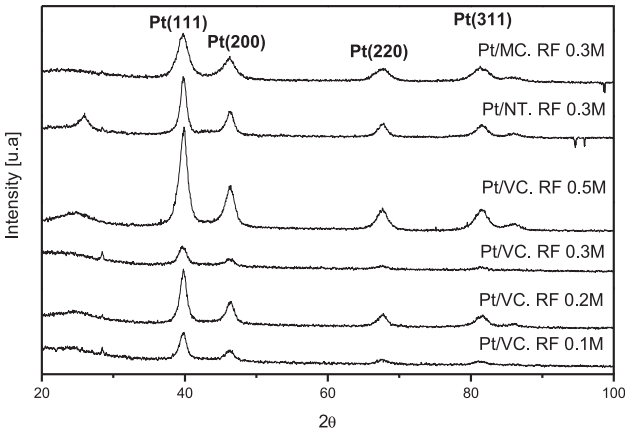

Fig. 5 – XRD of Pt/VC catalysts prepared with different concentrations of formic acid (between 0.1 and 0.5 M), Pt/NT and Pt/MC prepared by formic acid 0.3 M.

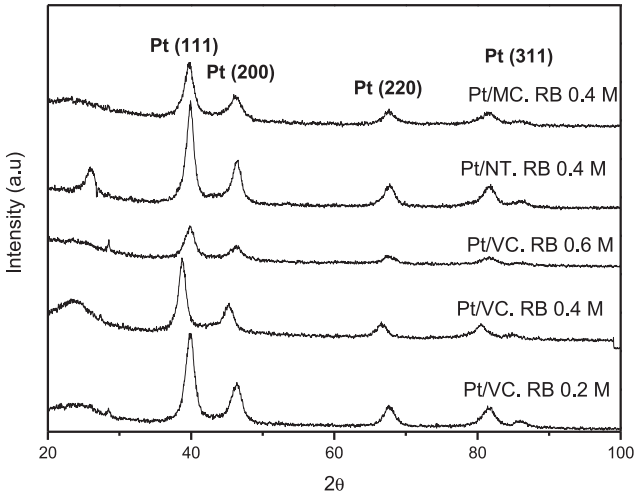

Fig. 6 – XRD of Pt/VC catalysts prepared with different concentrations of sodium borohydride (between 0.2 and 0.6 M), Pt/NT and Pt/MC prepared by $NaBH_4$ 0.4 M.

Table 4 – Particle diameter obtained by XRD (d_{XRD}) and values of metallic dispersion (obtained by H_2 chemisorption) for the different catalysts.

Catalysts	d_{XRD} (nm)	Dispersion (%)
Pt/VC. RF 0.1 M	7	24
Pt/VC. RF 0.2 M	7	14
Pt/VC. RF 0.3 M	4	39
Pt/VC. RF 0.5 M	7	17
Pt/VC. RB 0.2 M	6	34
Pt/VC. RB 0.4 M	6	34
Pt/VC. RB 0.6 M	8	36

similar tendencies both in metallic dispersion and in crystallite sizes determined by XRD than those obtained for catalysts prepared by reduction in liquid phase with formic acid or sodium borohydride. In this sense, the Pt/MC catalyst displays higher dispersion values than those supported on VC and NT. However, the electrochemical areas of the catalysts prepared by CI were much lower than the corresponding to the prepared by reduction in liquid phase (Table 5). The causes would be due to that an important portion of the active metal would be placed in the inner porous and it could not be electrochemically available, hence this impregnation technique (CI) would not be adequate for the preparation of Pt electrocatalysts supported on non-functionalized carbonaceous materials.

Finally some selected catalysts were characterized by Transmission Electronic Microscopy (TEM) in order to determine the distribution of metallic particles over each carbonaceous support. In this sense, the catalysts investigated (which displayed the best metallic dispersions and highest EASS values) were those supported on MC. TEM results for the Pt/MC catalyst prepared by reduction in liquid phase with sodium borohydride are in agreement with chemisorptions results, and they show a narrow distribution of Pt particles with mean diameters between 1.5 nm and 4 nm (with a mean diameter of 2.3 nm), such as observed in Fig. 11(a). The differences in metallic particle sizes with respect to XRD results could be attributed to that this technique could not detect very small particles.

Table 5 – Particle diameters (obtained from XRD), metallic dispersions (obtained by H_2 chemisorption) and electrochemically active specific surface (CO-stripping voltammetry) for different catalysts.

Catalyst	d_{XRD} (nm)	Dispersion (%)	Electrochemically active specific surface (m^2/g)
Pt/VC. RF 0.3 M	4	39	14
Pt/NT. RF 0.3 M	8	9	19
Pt/MC. RF 0.3 M	5	51	40
Pt/VC. RB 0.4 M	6	34	12
Pt/NT. RB 0.4 M	6	16	31
Pt/MC. RB 0.4 M	5	42	48
Pt/VC. CI.[a]	6	23	8.8
Pt/NT. CI.[a]	6	14	9
Pt/MC. CI.[a]	–	42	5.6

a Before the different characterizations, a reduction with H_2 at 230 °C was carried out.

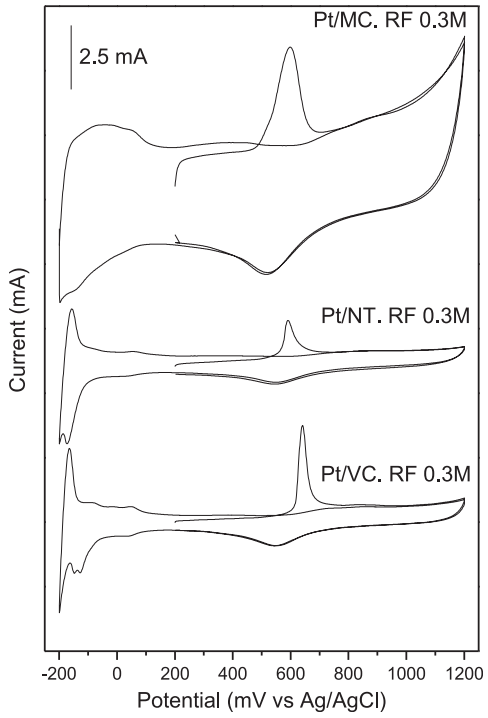

Fig. 7 – CO-stripping and conventional cyclic voltammetry for catalysts Pt/VC, Pt/NT and Pt/MC prepared by formic acid 0.3 M reduction in liquid phase.

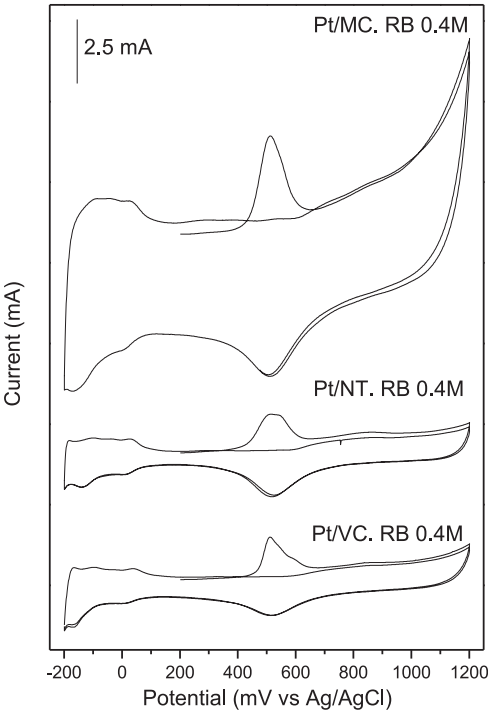

Fig. 8 – CO-stripping and conventional cyclic voltammetry for catalysts Pt/VC, Pt/NT and Pt/MC prepared by NaBH4 0.4 M reduction in liquid phase.

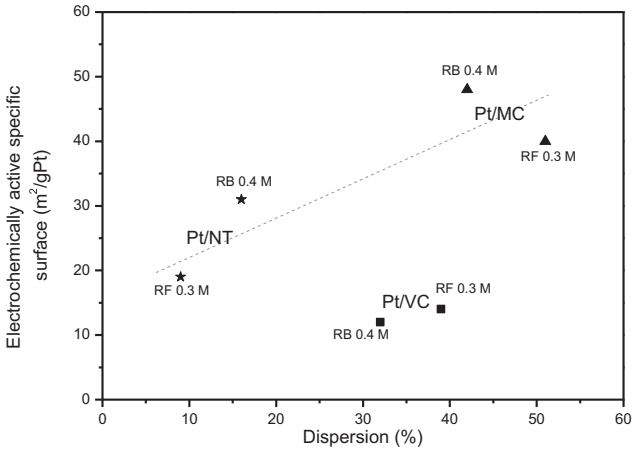

Fig. 9 – Electrochemically active specific surface as a function of the metallic dispersion calculated from hydrogen chemisorptions.

On the other hand the catalysts with the lowest electrochemical areas were those supported on the VC. TEM results corresponding to the catalyst prepared by the formic acid method show a very wide distribution of Pt particles, from 3 to 13 nm, and a mean particle diameter of 6.6 nm (see Fig. 11(b)). Besides the catalysts with intermediate EASS values were those supported on carbon nanotubes. Moreover TEM results for the Pt/NT catalyst prepared by reduction with sodium borohydride show a distribution narrower than for catalysts supported on Vulcan, and a mean particle diameter of about 5 nm (see Fig. 11(c)).

In conclusion, the excellent electrochemical performance of Pt catalysts supported on mesoporous carbon are due to the good interaction between Pt and the anchorage sites of this carbon which leads to very dispersed metallic particles with a very small mean diameter and a narrow distribution of particle sizes. Besides, suitable carbon supports for fuel cell catalysts have to combine a good electric conductivity to allow the flow of electrons, with a large and accessible surface area, and in this sense the mesoporous carbon displays an excellent

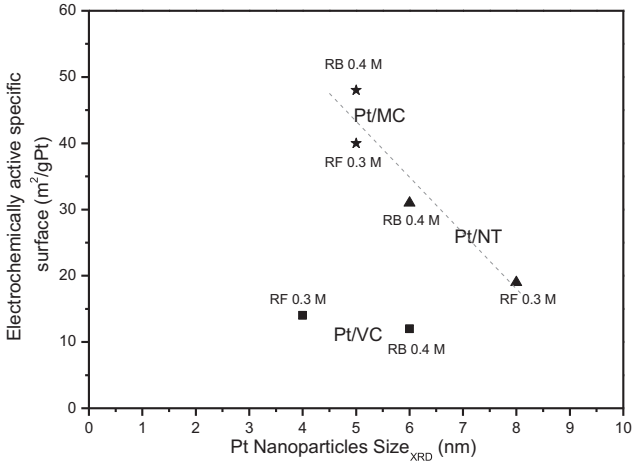

Fig. 10 – Electrochemically active specific surface as a function of the metallic particle diameter determined by XRD.

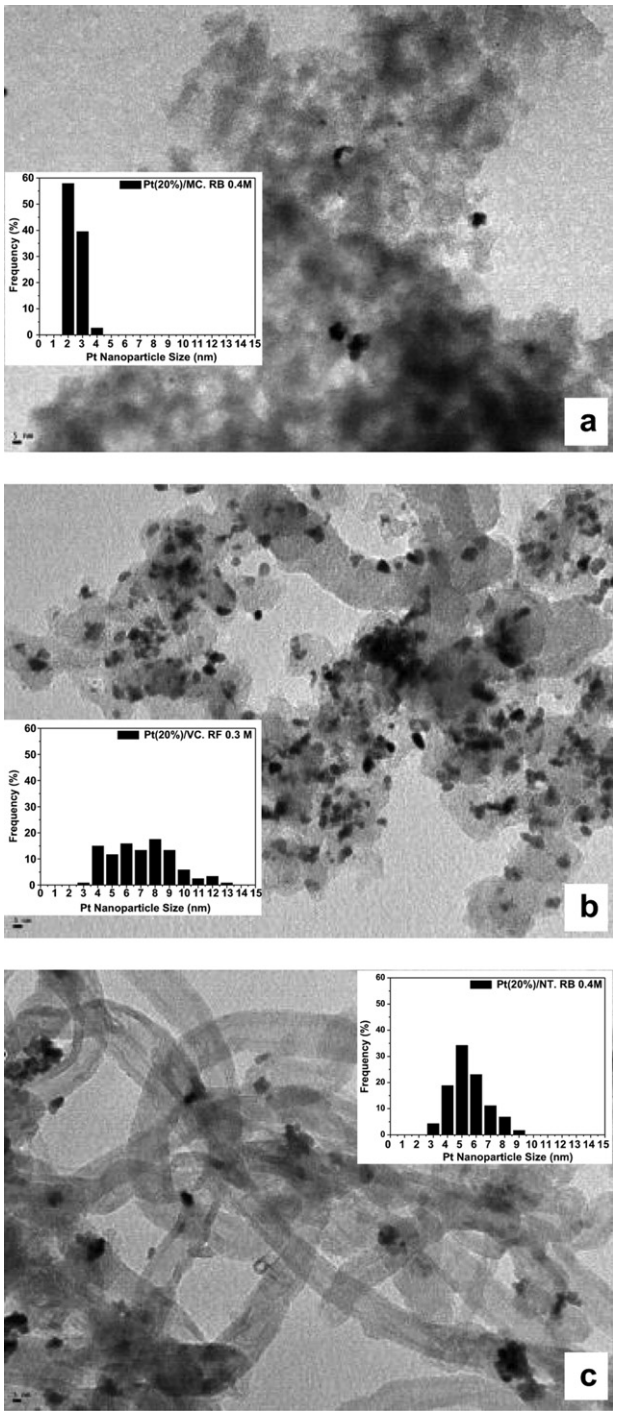

Fig. 11 – Distribution of particle diameters by TEM of (a) Pt/MC prepared by reduction with sodium borohydride (d = 2.3 nm). (b) Pt/VC prepared by reduction with formic acid (d = 6.6 nm). (c) Pt/NT prepared by reduction with sodium borohydride (d = 5.1 nm). The magnification scale was 5 nm.

electric conductivity [33] and, compared with the other supports, the highest surface area (about 400 m^2 g^{-1}). Our results are coincident with those of Raghuveer and Manthiram [34] who concluded that the enhanced activity of Pt/MC with respect to Pt/VC is due to the better dispersion and

utilization of the Pt catalysts, which are originated from a higher surface area and the meso-porosity. Vengatesan et al. [35] indicated also that the higher activity of the Pt/MC catalysts toward electrochemical reaction is due to the high dispersion of the Pt particles.

Other fact to take into account in the MC with VC and NT is the presence of moderate amounts of functional groups only on the MC, which could favor the metal–support interaction, thus leading to higher metallic dispersions and hence higher electrochemical performances [25,36]. Moreover, the porosity provides good physical anchoring sites for the deposited catalyst layer [37].

4. Conclusions

* The technique of deposition–reduction in liquid phase with formic acid or sodium borohydride for preparing a Pt (20 wt %)/VC guarantees a complete deposition of the metallic precursor on the carbonaceous support and an excellent reducibility degree of the metallic phase, thus avoiding reductive thermal treatments at high temperatures.
* The preparation of Pt catalysts by deposition–reduction in liquid phase using a concentration of formic acid equal to 0.3 M or a concentration of sodium borohydride of 0.2 or 0.4 M leads to catalysts with the highest dispersion and lowest particle sizes.
* The technique of conventional impregnation would not be adequate for the preparation of Pt catalysts with a high metallic content (20 wt%), thus showing that the impregnated Pt catalysts supported on VC, NT and MC without any functionalization treatment has very low EASS values.
* The electrochemical performance of supported Pt catalysts prepared by reduction in liquid phase is strongly dependent on the metallic dispersion, the particle size distribution and the nature of the carbonaceous material used as a support.
* The excellent behavior of MC as a support of Pt electrocatalysts are due to the good interaction between Pt and the anchorage sites of this carbon which leads to very dispersed metallic particles (very small mean diameter and a narrow distribution of particle sizes).

Acknowledgments

Authors thank to Universidad Nacional del Litoral (Project CAI+D), CONICET (Project 970/09) and ANPCYT (Projects 589/07 and PICT 2097, PAE 36985) for the financial support.

REFERENCES

[1] Srinivasan S. Fuel cells for extraterrestrial and terrestrial applications. J Electrochem Soc 1989;136:41C–8C.
[2] Yi B, Yu H, Hou Z, Lin Z, Zhang J, Ming P, et al. Electrocatalysts for proton exchange membrane fuel cells. Chinese Academy of Sciences. Precious Metal 2002;23:1–7.
[3] Ticianelli EA, Berry JG, Srinivasan S. Dependence of performance of solid polymer electrolyte fuel cells with low platinum loading on morphologic characteristics of the electrodes. J Appl Electrochem 1991;21:597–605.
[4] Lee SJ, Mukerjee S, McBreen J, Rho YW, Kho YT, Lee TH. Effects of Nafion impregnation on performances of PEMFC electrodes. Electrochim Acta 1998;43:3693–701.
[5] Costamagna P, Srinivasan S. Quantum jumps in the PEMFC science and technology from the 1960s to the year 2000. Part I. Fundamental science aspects. J Power Sources 2001;102:242–52.
[6] Gonzalez ER, Ticianelli EA, Pinheiro ALN, Perez J. Processo de obtencão de catalisador de platina dispersa ancorada em substrato através da reducão por ácido. Brazilean patent INPI 003121; 1997.
[7] Lizcano-Valbuena WH, Paganin VA, Gonzalez ER. Methanol electro-oxidation on gas diffusion electrodes prepared with Pt–Ru/C catalysts. Electrochim Acta 2002;47:3715–22.
[8] Nores-Pondal FJ, Vilella IMJ, Troiani H, Granada M, de Miguel SR, Scelza OA, et al. Catalytic activity vs. size correlation in platinum catalysts of PEM fuel cells prepared on carbon black by different methods. Int J Hydrogen Energy 2009;34:8193–203.
[9] Salgado JRC, Gonzalez ER. Correlation between catalytic activity and particle size of Pt/C prepared by different methods. Eclet Quim 2003;28:77–85.
[10] Salgado JRC, Antolini E, Gonzalez ER. Pt–Co/C Electrocatalysts for oxygen reduction in H_2/O_2 PEMFCs synthesized by borohydride method. J Electrochem Soc 2004;151:A2143–9.
[11] Xing Y. Synthesis and electrochemical characterization of uniformly-dispersed high loading Pt nanoparticles on sonochemically-treated carbon nanotubes. J Phys Chem B 2004;108:19255–9.
[12] Zhang J, Wang X, Wu C, Wang H, Yi B, Zhang H. Preparation and characterization of Pt/C catalysts for PEMFC cathode: effect of different reduction methods. React Kinetic Catal Lett 2004;83:229–36.
[13] Wang ZB, Zhao CR, Shi PF, Yang YS, Yu ZB, Wang WK, et al. Effect of a carbon support containing large mesopores on the performance of a Pt–Ru–Ni/C catalyst for direct methanol fuel Cell. J Phys Chem C 2010;114:672–7.
[14] de Miguel SR, Vilella JI, Jablonski EL, Scelza OA, Salinas Martínez de Lecea C, Linares-Solano A. Preparation of Pt catalysts supported on activated carbon felts (ACF). Appl Catal A Gen 2002;232:237–46.
[15] Liu Z, Gan LM, Hong L, Chen W, Lee JY. Carbon-supported Pt nanoparticles as catalysts for proton exchange membrane fuel cells. J Power Sources 2005;139:73–8.
[16] Nores Pondal FJ. Doctoral thesis. Buenos Aires-Argentina: CNEA; 2009.
[17] Prabhuram J, Wang X, Hui CL, Hsing I. Synthesis and characterization of surfactant-stabilized Pt/C nanocatalysts for fuel cell applications. J Phys Chem B 2003;107:11057–64.
[18] Bruno MM, Cotella NG, Miras MC, Barbero C. A novel way to maintain resorcinol-formaldehyde porosity during drying: stabilization of the sol–gel nanostructure using a cationic polyelectrolyte. Colloids Surf A 2010;362:28–32.
[19] Bruno MM, Corti HR, Balach J, Cotella GN, Barbero CA. Hierarchical porous materials: capillaries in nanoporous carbon. Funct Mater Lett 2009;2:135–8.
[20] Benson JE, Boudart M. Hydrogen–oxygen titration method for the measurement of supported platinum surface areas. J Catal 1965;4:704–71.
[21] Takasu Y, Kawaguchi T, Sugimoto W, Murakami Y. Effects of the surface area of carbon support on the characteristics of highly dispersed Pt–Ru particles as catalysts for methanol oxidation. Electrochim Acta 2003;48:3861–8.
[22] Boehm HP. Some aspects of the surface chemistry of carbon blacks and other carbons. Carbon 1994;32:759–69.

[23] Roman-Martinez MC, Cazorla-Amoros D, Linares-Solano A, Salinas-Martinez de Lecea C, Yamashita H, Anpo M. Metal-support interaction in Pt/C catalysts. Influence of the support surface chemistry and the metal precursor. Carbon 1995;33:3–13.
[24] de Miguel SR, Scelza OA, Roman-Martinez MC, Salinas-Martinez de Lecea C, Cazorla-Amoros D, Linares-Solano A. States of Pt in Pt/C catalyst precursors after impregnation, drying and reduction steps. Appl Catal A Gen 1998;170:93–103.
[25] Fraga MA, Jordão E, Mendesa MJ, Freitas MMA, Faria JL, Figueiredo JL. Properties of carbon-supported platinum catalysts: role of carbon surface sites. J Catal 2002;209:355–64.
[26] Solhy A, Machado BF, Beausoleil J, Kihn Y, Gonçalves F, Pereira MFR, et al. MWCNT activation and its influence on the catalytic performance of Pt/MWCNT catalysts for selective hydrogenation. Carbon 2008;46:1194–207.
[27] de Miguel SR, Roman-Martınez MC, Jablonski EL, Fierro JLG, Cazorla-Amoros D, Scelza OA. Characterization of bimetallic PtSn catalysts supported on purified and H_2O_2-functionalized carbons used for hydrogenation reactions. J Catal 1999;184:514–25.
[28] Wagner CD, Riggs WM, Davis LE, Moulder JF, Muilenberg GE. Handbook of X-ray photoelectron spectroscopy. Perkin-Elmer CO: Physical Electronics; 1979.
[29] Shukla AK, Neergat M, Bera P, Jayaram V, Hegde MS. An XPS study on binary and ternary alloys of transition metals with platinized carbon and its bearing upon oxygen electroreduction in direct methanol fuel cells. J Electroanalytical Chem 2001;504:111–9.
[30] Prabhuram J, Zhao TS, Wong CW, Guoet JW. Synthesis and physical/electrochemical characterization of Pt/C nanocatalyst for polymer electrolyte fuel cells. J Power Sources 2004;134:1–6.
[31] Sevilla M, Sanchís C, Valdés-Solís T, Morallon E, Fuertes AB. Highly dispersed platinum nanoparticles on carbon nanocoils and their electrocatalytic performance for fuel cell reactions. Electrochim Acta 2009;54:2234–8.
[32] Maillard F, Eikerling M, Cherstiouk OV, Schreier S, Savinova E, Stimming U. Size effects on reactivity of Pt nanoparticles in CO monolayer oxidation: the role of surface mobility. Faraday Discuss 2004;125:357–77.
[33] Antolini E. Carbon supports for low-temperature fuel cell catalysts. Appl Catal B Environ 2009;88:1–24.
[34] Raghuveer V, Manthiram A. Mesoporous carbon with larger pore diameter as an electrocatalyst support for methanol oxidation. Electrochem Solid-State Lett 2004;7:A336–9.
[35] Vengatesan S, Kim HJ, Kim SK, Oh IH, Lee SY, Cho EA, et al. High dispersion platinum catalyst using mesoporous carbon support for fuel cells. Electrochim Acta 2008;54:856–61.
[36] Chen W, Xin Q, Sun G, Wang Q, Mao Q, Su H. The effect of carbon support treatment on the stability of Pt/C electrocatalysts. J Power Sources 2008;180:199–204.
[37] Bruno MM, Franceschini EA, Planes GA, Corti HR. Electrodeposited platinum catalysts over hierarchical carbon monolithic support. J Appl Electrochem 2010;40:257–63.